Journal of Reproduction and Development, Vol. 65, No 1, 2019

—Original Article—

Destabilization of spindle assembly checkpoint causes aneuploidy during meiosis II in murine post-ovulatory aged oocytes

Gaku SHIMOI[1)], Masaru TOMITA[1)], Marino KATAOKA[1)] and Yuichi KAMEYAMA[1)]

[1)]*Laboratory of Animal Resources and Development, Department of Northern Biosphere Agriculture, Faculty of Bioindustry, Tokyo University of Agriculture, Hokkaido 099-2493, Japan*

Abstract. Mammalian oocyte quality degrades over time after ovulation *in vitro*, which can cause fatal defects such as chromosomal aneuploidy. As various oocyte manipulations employed in assisted reproductive technology are time consuming, post-ovulatory aging is a serious problem to overcome in reproductive medicine or ova research. In this study, we investigated the effects of postovulatory aging on the incidence of chromosome aneuploidy during meiosis II, with a focus on the expression of functional proteins from the spindle assembly checkpoint (SAC). Chromosome analysis was used to assess the rate of aneuploidy in *in vitro* aged oocytes, or in early embryos derived from aged oocytes. Immunofluorescent staining was used to detect the localization of MAD2, which is a SAC signal that monitors the correct segregation of sister chromatids. Immunoblotting was used to quantify cohesin subunits, which are adhesion factors connecting sister chromatids at the metaphase II (MII) centromere. It was shown that post-ovulatory oocyte aging inhibits MAD2 localization to the sister kinetochore. Furthermore, oocyte aging prevented cohesin subunits from being maintained or degraded at the appropriate time. These data suggest that the destabilization of SAC signaling causes sister chromatid segregation errors in MII oocytes, and consequently increases the incidence of aneuploidy in early embryos. Our findings have provided distinct evidence that the post-ovulatory aging of oocytes might also be a risk factor for aneuploidy, irrespective of maternal age.

Key words: Aneuploidy, Cohesin, MAD2, Postovulatory aging, Spindle assembly checkpoint

(**J. Reprod. Dev. 65:** 57–66, 2019)

In recent years, the importance of oocyte aging in reproductive health has been widely acknowledged. Oocyte aging leads to alterations to cytoplasmic organelles at the molecular level, and has a negative impact on embryo or fetal development after fertilization. Various kinds of alterations, such as a functional deterioration of mitochondria [1, 2], failed intracellular calcium control by endoplasmic reticulum [3, 4], and abnormalities in genomic imprinting mechanisms [5, 6] have previously been reported. These alterations, caused by oocyte aging, have often been considered signs of deterioration in oocyte quality. It is well known that chromosomal aneuploidy is a consequence of functional loss caused by oocyte aging [7–9]. Chromosomal aneuploidy in oocytes, which is a major cause of decreased developmental competence and loss of pregnancy [8–13], is caused by chromosomal segregation errors, such as early segregation and non-disjunction during meiosis. Recent molecular research into chromosomal instability has progressed rapidly, and advanced the general understanding.

Spindle assembly checkpoint (SAC), which functions during cell division, is one of the checkpoint mechanisms functional during the cell cycle. SAC is a monitoring system, which equally distributes chromosomes by correctly attaching spindle microtubules to the chromosome kinetochore [14, 15] (Fig. 1). MAD2, which binds with MAD1 on the chromosome kinetochore, monitors the connection between the microtubule of the spindle fiber and the kinetochore. When there is a kinetochore that is not fully connected to a spindle fiber, MAD2 localizes and sends a signal to inhibit the progression of anaphase [16]. This signal is released when the chromosomes are attached with spindle microtubules and aligned on the equatorial plane. Cohesin, a multiprotein complex that is a component of SAC, acts as an adhesion factor to keep homologous chromosomes and sister chromatids together until the completion of meiosis I and II, respectively [17]. In mammals, meiotic cohesin complexes consist of four evolutionarily conserved protein subunits: two members of the structural maintenance of chromosomes (SMC) family (SMC1β and SMC3), a member of the Kleisin family (REC8), and stromal antigen (SA) subunit (SA3). SMC proteins, which constitute a core subunit of the cohesin complex, regulate higher-order chromosome structure and function. REC8, which contains a cleavage recognition site for separase, has a role in maintenance of chromosome cohesion with SA3 [18] and SMC proteins. Chromosome cohesion, mediated by cohesin proteins, which form a ring-like protein structure, is established at the chromosome centromere and along the chromosome arms [17, 18]. The release of SAC induces a degradation of cyclin B and securin, which follows the activation of anaphase-promoting complex/cyclosome (APC/C), which serves as an ubiquitin ligase. CDC20, which is an APC/C activator, inhibits the activity of APC/C to form a M-phase checkpoint complex with MAD2 and BubR1 [15]. Securin is a separase inhibitor protein and its ubiquitination by APC/C promotes cohesin detachment following the activation of separase, which subsequently induces segregation of homologous

Received: April 16, 2018
Accepted: November 2, 2018
Published online in J-STAGE: November 22, 2018

Corresponence: G Shimoi (e-mail: g1shimoi@nodai.ac.jp)

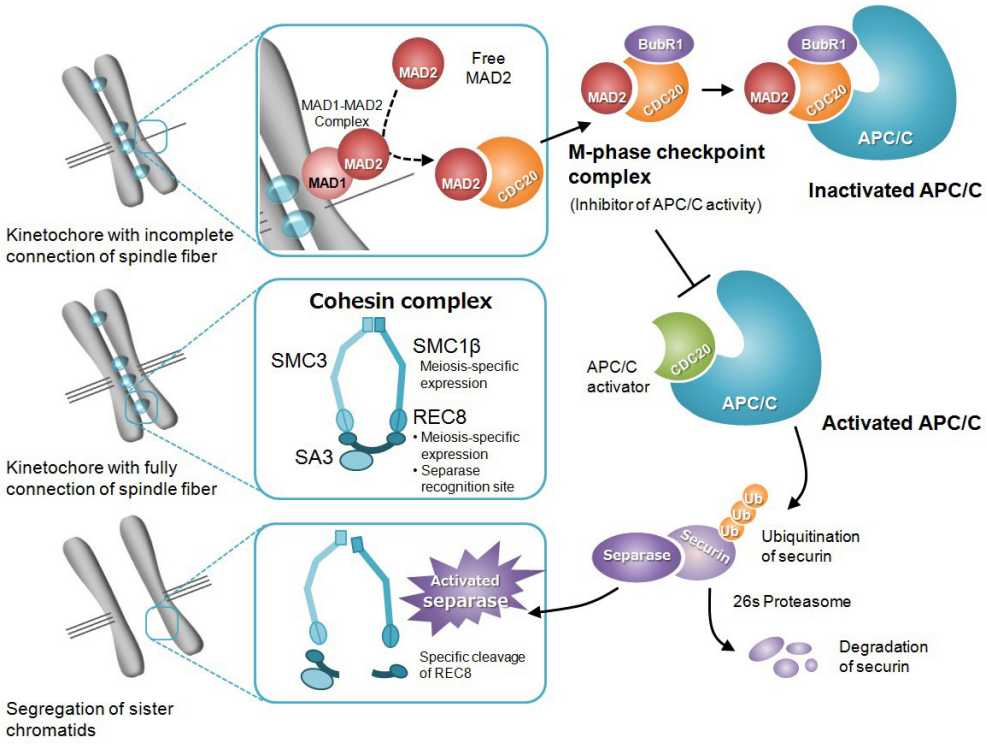

Fig. 1. Summary of the molecular mechanism of spindle assembly checkpoint. MAD2, which binds with MAD1 on the kinetochore, monitors the connection between a spindle fiber and kinetochore. The MAD1-MAD2 complex serves as a catalyst to promote binding between a free MAD2 and CDC20. The MAD2-CDC20 complex forms a M-phase checkpoint complex (MCC) with other functional proteins, and suppresses the activity of APC/C. A fully connected spindle fiber on the kinetochore interrupts the signal from the spindle checkpoint. CDC20, released from MCC, behaves as an APC/C activator by binding with APC/C. Activated APC/C promotes ubiquitination of securin, which regulates separase activity. The separase activated by securin degradation cleaves REC8, which is contained in the cohesin complex. Finally, sister chromatids lose cohesin, an adhesion factor, and are segregated by tension from the spindle fiber.

chromosomes and sister chromatids (Fig. 1) [17].

Many reports suggest the relation between oocyte aging and SAC processes, including chromosome cohesion [19–25]. In humans, the inter-kinetochore distance between sister chromatids significantly increases in oocytes as maternal age advances, suggesting that sister chromatid cohesion has weakened [20, 23]. Expression of meiosis-specific REC8, a cohesin subunit, has also been shown to decrease as maternal age advances [19, 23]. It is suggested that these factors cause incidences of unpaired sister chromatids and early chromatid segregation, leading to the induction of aneuploidy. Most studies investigating chromosome segregation errors that occur during meiosis I focus on the effect of pre-ovulatory maternal age [7, 9, 19–22]. To gain insight into oocyte aging, the aging process needs to be considered on two different axes of time. One is maternal aging, which involves an inter-annual change in oocytes that advances with age. This is also described as pre-ovulatory aging, which progresses in the ovary. The other is post-ovulatory aging, or the temporal alterations in oocytes that have been induced to ovulate by ovarian stimulation in response to a luteinizing hormone or a chorionic hormone. Post-ovulatory aging progresses in the oviduct or can be induced *in vitro*. Although mature oocytes arrested at metaphase II (MII) fertilize immediately after ovulation, the optimal time of fertilization (fertilization window) varies depending on the species [8]. If fertilization is not completed successfully during the ideal fertilization window, the ovulated oocytes will be retained in the oviduct, or cultivated in a culture dish. The quality of these unfertilized oocytes deteriorates in a time-dependent manner [8]. As the *in vitro* manipulation time for ovulated oocytes used in reproductive medicine and ova research lengthens, post-ovulatory oocyte aging would become a problem that must be overcome.

This study aims to investigate chromosomal aneuploidy induced by post-ovulatory aging during meiosis II, with a focus on chromosomal segregation errors and expression of functional SAC proteins.

Materials and Methods

Animals

ICR male (10–15 weeks old) and female (8–10 weeks old) mice were used for experiments described below. The mice were maintained under controlled light conditions (14 h light from 0600 h to 2000 h; 10 h dark) and temperature (24 ± 2°C). All procedures involving animal experiments were conducted according to guidelines approved by the Animal Research Committee of Tokyo University of Agriculture.

Oocyte collection and in vitro aging

To obtain MII oocytes, female mice were induced to super-ovulate

by consecutive injection of 5 IU pregnant mare serum gonadotropin (ASKA Animal Health, Tokyo, Japan) and 5 IU human chorionic gonadotropin (hCG; ASKA Animal Health) at 48 h intervals. The super-ovulated mice were euthanized 15 h after the hCG injection, and the oviductal ampullae were broken to release the cumulus-oocyte complexes (COCs) into TYH medium under paraffin liquid (Nacalai Tesque, Kyoto, Japan). The collected COCs were incubated for a certain time at 37.5°C in a humidified atmosphere with 5% CO_2 and used as *in vitro* aged oocytes. In this study, two experimental groups were designated. One was an aged group, where oocytes incubated for 6 or 12 h *in vitro* after oocyte collection were examined. The other was a fresh group, which functioned as a control, where oocytes were immediately examined after collection.

Oocyte activation

Oocytes were freed from cumulus cells by brief exposure to 0.1% hyaluronidase (Sigma Chemical, St. Louis, MO, USA) in Hepes-buffered CZB medium (H-CZB) at 37.5°C, followed by washes and subsequent activation treatment. The denuded oocytes were incubated in activating medium for 1 h at 37.5°C in a humidified atmosphere with 5% CO_2. Ca^{2+}-free H-CZB supplemented with 10 mM strontium chloride ($SrCl_2$, Kanto Chemical, Tokyo, Japan) was used as activating medium. After the $SrCl_2$ treatment, oocytes were incubated in normal H-CZB. Six hours after the onset of activation treatment with $SrCl_2$, oocytes with one pronucleus were considered activated, and were examined for chromosome analysis or immunoblotting.

In vitro fertilization (IVF)

To perform chromosome analysis at the 8-cell stage, IVF was performed using COCs obtained from oviductal ampullae. Before insemination, spermatozoa were collected from one cauda epididymis and pre-cultured in TYH medium for 1.5 h at 37°C in a humidified atmosphere with 5% CO_2. Insemination was performed with a final sperm concentration of 1×10^5/ml in a droplet of TYH medium. After co-incubation for six hours, oocytes with two distinct pronuclei and a second polar body were considered fertilized. These fertilized oocytes were transferred into a droplet of KSOM medium supplemented with essential and non-essential amino acids (Gibco, Grand Island, NY, USA) (mKSOM), and were then cultured for 56 h at 37°C in a humidified atmosphere with 5% CO_2. Some of these embryos were maintained in culture for up to 96 h in order to assess developmental capacity.

Chromosome analysis

Chromosome analysis was performed on both oocytes and 8-cell stage embryos. To eliminate the male genome factor, chromosome analysis of oocytes was performed after activating treatment by $SrCl_2$ without fertilization. After the activation treatment, oocytes were cultured in mKSOM for 20 h. Six hours before termination of the culture, the activated oocytes were treated with mKSOM supplemented with 0.1 μg/ml demecolcine (Wako Pure Chemical Industries, Osaka, Japan). Chromosome spreads were prepared according to the method reported by Yoshizawa *et al*. [26, 27], with slight modification. The slides were stained for 15 min with 4% Giemsa solution (Merck Millipore, Darmstadt, Germany). Stained chromosome spreads were observed with an optical microscope and the number of chromosomes was counted. Chromosome spreads with more or less than 40 chromosomes, or showing polyploidy, were considered as numerical chromosome aberrations (NCAs). Some 8-cell embryos, which were cultured for 56 h after IVF, were also examined for chromosome analysis with a similar method.

Immunofluorescent staining

The morphological observation of spindles and the localization analysis of MAD2 protein in MII oocytes were performed using immunofluorescent staining. To detect normal MAD2 localization on the chromosome kinetochore, oocytes were incubated in mKSOM supplemented with 20 μg/ml nocodazole (Sigma), as an inhibitor of microtubule polymerization, for 30 min at 37°C. The zona pellucida was removed from the oocytes with washes in Dulbecco's phosphate-buffered saline (D-PBS) containing 0.5% pronase (Merck Millipore) for 5 min at 37°C, and fixed with 4% paraformaldehyde (Wako) in D-PBS for 30 min at room temperature. After fixation, the oocytes were treated with 1% TritonX-100 (Wako) in D-PBS for 15 min at room temperature, and were washed three times with D-PBS. The permeabilized oocytes were blocked in 3% bovine serum albumin (Sigma) for 30 min at room temperature. After washing thrice with D-PBS, the oocytes were incubated with goat anti-MAD2 antibody (1:50 dilution, Santa Cruz Biotechnology, Dallas, TX, USA) as a primary antibody over night at 4°C and then washed three times with D-PBS. This was followed by incubation in Alexa Fluor® 594-conjugated anti-goat IgG secondary antibody (1:500 dilution, Invitrogen) for 60 min. After washing thrice with D-PBS, the oocytes were incubated with mouse anti-α-Tubulin monoclonal antibody (1:500 dilution, Sigma) as a primary antibody for 60 min at room temperature, washed thrice with D-PBS, then incubated in fluorescein isothiocyanate (FITC)-conjugated anti-mouse IgG (1:100 dilution, Sigma) as a secondary antibody for 1 h at room temperature. Oocyte chromosomes were stained with 0.1 μg/ml 4',6-diamidino-2-phenylindole (DAPI, Sigma) for 30 min at 4°C. Following washing, the oocytes were mounted on glass slides, covered with glass cover slips, and observed under 200–400 times magnification using a fluorescence microscope system, BX51 and DP71 (Olympus, Tokyo, Japan).

Immunoblotting

The expression of cohesin subunits and functional proteins of SAC was detected in activated or non-activated (MII) oocytes using immunoblotting. Forty oocytes per tube were lysed in RIPA buffer (Wako) supplemented with a protease inhibitor cocktail (Thermo Fisher Scientific, Yokohama, Japan) and incubated on ice for 10 min. After being centrifuged at 12,000 × *g* for 5 min at 4°C, the oocyte lysates were frozen at –80°C until use. The oocyte lysates were diluted with an equal volume of 2 × Laemmli sample buffer (Bio-Rad, Hercules, CA, USA) containing 5% 2-mercaptoethanol (Wako) and heated to 100°C for 5 min. Proteins were separated using sodium dodecyl sulfate polyacrylamide gel electrophoresis (SDS-PAGE) with a stacking gel containing 4% acrylamide (Wako) and a separating gel containing 7.5~10% acrylamide run for 50 min at 200 V. Proteins were then electrophoretically transferred onto polyvinylidene difluoride (PVDF) membranes (GE Healthcare, Chicago, IL, USA) for 30 min at 15 V. Each membrane was blocked with PVDF blocking reagent

Table 1. Ability of pronucleus formation in mouse post-ovulatory aged oocytes after SrCl2 activation

Exp. group	Time of *in vitro* aging	No. of oocytes treated	No. (%) of pronuclear oocytes			
			Dead	Activated		Without a PN
				2 PN	1 PN	
Fresh	0 h	114	6 (5.3) [b]	0 (0.0)	101 (88.6)	7 (6.1)
Aged	6 h	97	5 (5.2) [b]	2 (2.0)	83 (85.6)	7 (7.2)
	12 h	117	27 (23.1) [a]	0 (0.0)	82 (70.1)	8 (6.8)

Values with different superscripts in the same column are significantly different ($P < 0.05$).

Table 2. Preimplantation development of mouse post-ovulatory aged oocytes after IVF

Exp. group	Time of *in vitro* aging	No. of oocytes examined	No. (%) of oocytes fertilized	No. of embryos cultured	No. (%)* of embryos developed to		
					Blastocyst	Arrested	Degenerated
Fresh	0 h	210	181 (86.2) [b]	104	91 (87.5) [b]	9 (8.7)	4 (3.8) [b]
Aged	6 h	228	200 (87.7) [b]	105	84 (80.0)	10 (9.5)	11 (10.5)
	12 h	247	193 (78.1) [a]	113	82 (72.6) [a]	14 (12.4)	17 (15.0) [a]

Values with different superscripts in the same column are significantly different ($P < 0.05$). * Percentage of cultured embryos.

(TOYOBO, Osaka, Japan) for 1 h at room temperature followed by incubation overnight at 4°C in goat anti-SMC1β antibody (1:1,000 dilution, Santa Cruz), rabbit anti-SMC3 antibody (1:2,000 dilution, Cell Signaling Technology, Danvers, MA, USA), rabbit anti-REC8 antibody (1:2,000 dilution, Bioss Antibody, Woburn, MA, USA), rabbit anti-Securin/PTTG antibody (1:1,000 dilution, Bioss), rabbit anti-CDC20 antibody (1:1,000 dilution, CST), or goat anti-MAD2 antibody (1:1,000 dilution, Santa Cruz) as a primary antibody. The membranes were then washed three times with PBS containing 1% Tween 20 (PBS-T) and incubated with a horseradish peroxidase (HRP)-conjugated anti-goat IgG (1:4,000 dilution, Santa Cruz) or anti-rabbit IgG (1:4,000 dilution, GE Healthcare) secondary antibody for 1 h at room temperature. The membranes were washed thrice with PBS-T and proteins were detected using an ECL Prime western blotting detection kit (GE Healthcare). After detection of target proteins, the membranes were washed twice and re-blocked. As an internal control, the expression of β-actin was detected as described above using mouse anti-β-actin antibody (1:1,000 dilution, Wako) as a primary antibody and HRP-conjugated anti-mouse IgG secondary antibody (1:4,000 dilution, GE Healthcare). ImageJ was used to quantify the intensity of the protein bands of interest, and band intensities were normalized to an internal control.

Statistical analysis

The Chi-square test was used to determine the statistical significance of the percentages of activation, fertilization, development, and NCAs. The Tukey-Kramer test of multiple comparison following one-way ANOVA was used to compare the average expression levels of proteins among the groups. A P value < 0.05 was considered significant.

Results

Pronuclear formation after oocyte activation

The rates of pronuclear formation in the post-ovulatory aged oocytes are shown in Table 1. Normal activated oocytes which have one pronucleus were observed in 85.6% (83/97) and 70.1% (82/117) of all treated oocytes in the 6 and 12 h aged groups respectively, and 88.6% (101/114) in the fresh group. The rates of dead oocytes after activation treatment were 5.2% (5/97) and 23.1% (27/117) in the 6 and 12 h aged groups respectively, and the rate of dead oocytes in the 12 h aged group was significantly higher than that in the 6 h aged group and the fresh group (5.3%, 6/114) ($P < 0.05$).

Preimplantation development after IVF

The fertilization and developmental rates in the post-ovulatory aged oocytes are shown in Table 2. Fertilized oocytes were recognized in 87.7% (200/228) and 78.1% (193/247) of all examined oocytes in the 6 and 12 h aged groups, respectively, and the fertilization rate in the 12 h aged group was lower than that in the 6 h aged group and the fresh group (86.2%, 181/210) ($P < 0.05$). Embryos that developed to the blastocyst stage were observed in 80.0% (84/105) and 72.6% (82/113) of all cultured embryos in the 6 and 12 h aged groups, respectively, and the developmental rate in the 12 h aged group was lower than that in the fresh group (87.5%, 91/104) ($P < 0.05$).

Numerical chromosome aberration in oocytes and early embryos

The rates of NCAs in the post-ovulatory aged oocytes completing second meiosis are shown in Fig. 2A. NCAs were detected in 26.2% (11/42) and 40.0% (16/40) of all observed chromosome spreads in the 6 and 12 h aged groups, respectively, and numbers of NCAs in the 12 h aged group were significantly higher than that in the fresh group (17.2%, 5/29) ($P < 0.05$). Most of the NCAs observed in oocytes indicated aneuploidy (23.8, 40.0% in 6 and 12 h aged groups respectively, and 10.3% in the fresh group). The rates of NCAs in 8-cell embryos derived from the aged oocytes are shown in Fig. 2B. NCAs were detected in 35.6% (36/101) and 51.5% (35/68) of all observed chromosome spreads in the 6 and 12 h aged groups, respectively, and the 12 h aged group had significantly more NCAs

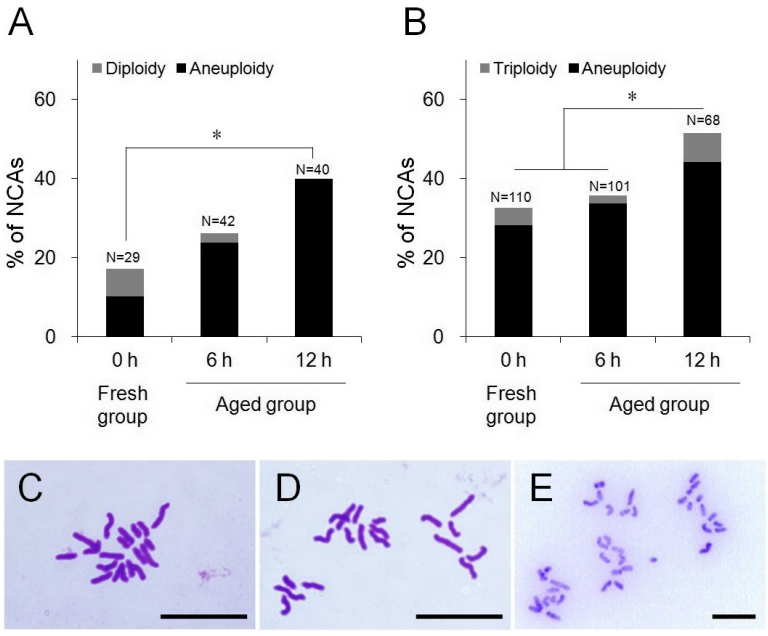

Fig. 2. Comparison of the frequency of NCAs between aged and fresh groups. (A) Frequency of NCAs in mouse oocytes. (B) Frequency of NCAs in mouse 8-cell embryos. (C) Normal chromosome spread in mouse oocyte (n = 20). (D) Chromosome spread which shows aneuploidy in mouse oocyte (n = 19). (E) Chromosome spread which shows diploidy in mouse oocyte (n = 40). Scale bar = 10 μm. * $P < 0.05$.

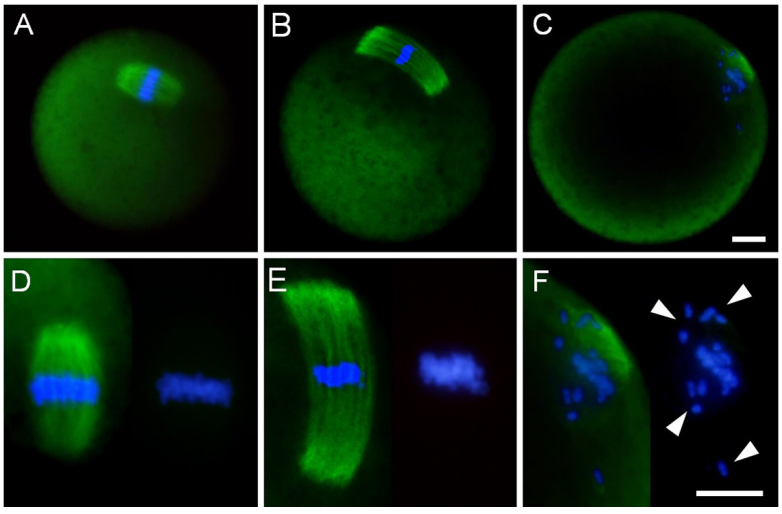

Fig. 3. Spindle shape and chromosome alignment in mouse MII oocytes. (A) Fresh oocytes, which were immediately collected at 15 hours after hCG administration. (B, C) Aged oocytes, which were cultured for 12 h in medium following oocyte collection. (D–F) Higher magnified images of spindle (left) and chromosome alignment (right). White arrowheads indicate chromosome misalignment. Immunofluorescent staining of α-tubulin (green). DNA (blue) was stained with DAPI. Scale bar = 10 μm.

than the 6 h aged and the fresh groups (32.7%, 36/110) ($P < 0.05$). As with the oocytes, most NCAs discovered in 8-cell embryos indicated aneuploidy (33.7, 44.1% in the 6 and 12 h aged groups, respectively, and 28.2% in the fresh group).

Morphology of MII spindle

Chromosome analysis indicated that the NCAs detected in the early embryos derived from aged oocytes might be attributed to a failure during the chromosomal segregation step of meiosis II. To observe spindle shapes at the MII stage, oocyte spindles were visualized by immunofluorescent staining. The MII spindles of fresh oocytes were barrel-shaped and slightly pointed (Fig. 3A). In contrast, the spindles of aged oocytes were elongated, and the pole width of the spindles was wider than that observed in fresh oocytes (Fig. 3B).

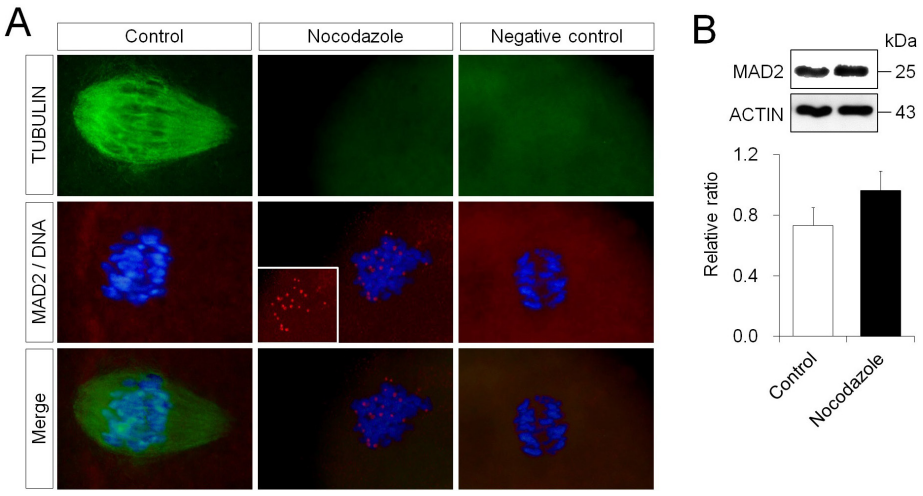

Fig. 4. Localization and expression level of MAD2 in fresh mouse oocytes with blocked microtubule polymerization. (A) Immunofluorescent staining of MAD2 (red) and α-tubulin (green). DNA (blue) was stained with DAPI. D-PBS, instead of the primary antibody, was used as the negative control. The inserted panel in the middle panel of the nocodazole group indicates only MAD2 signals. Scale bar = 10 μm. (B) Western blotting and expression levels of MAD2 in oocytes treated with nocodazole. β-actin was used as a loading control.

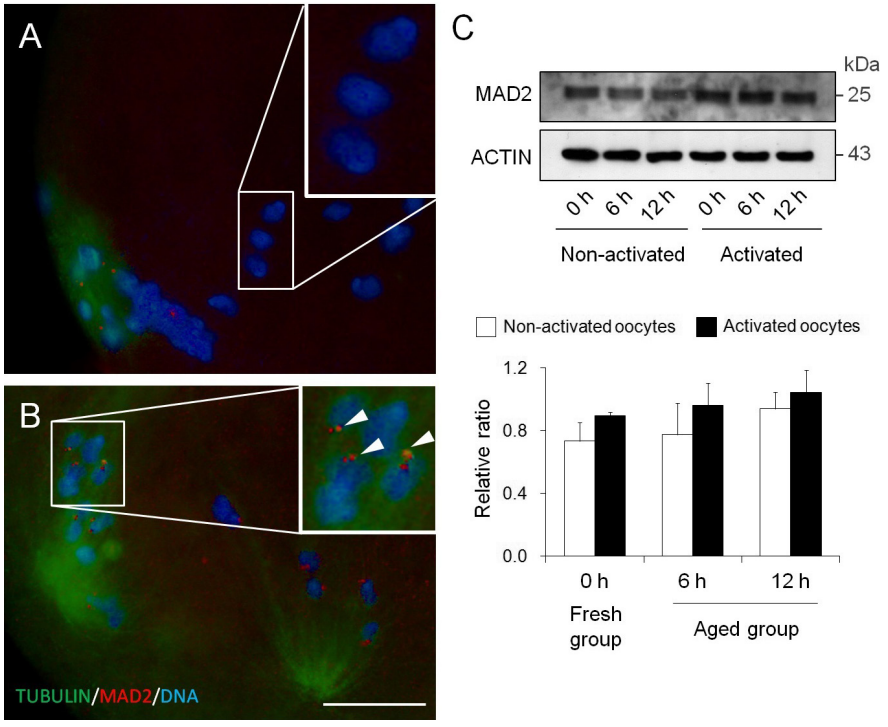

Fig. 5. Localization and expression level of MAD2 in mouse post-ovulatory aged oocytes. (A, B) Immunofluorescent staining of MAD2 (red) and α-tubulin (green) in 12 h aged oocytes. DNA (blue) was stained with DAPI. (A) No signal of MAD2 on the misaligned chromosome. (B) MAD2 localization on the chromosome, despite spindle fiber connections to kinetochores. The white arrowheads indicate MAD2 localization at the chromosome kinetochore. Scale bar = 10 μm. (C) Western blotting and expression levels of MAD2 in aged oocytes.

Furthermore, some of the aged oocytes had obscured spindles and misaligned chromosomes (Fig. 3C). It is possible that post-ovulatory aged oocytes have difficulty maintaining spindle morphology and the connection between the spindle and chromosome.

Expression of MAD2

Initially, for the purpose of detecting the normal localization of MAD2, kinetochores without microtubule connections were produced artificially by blocking the polymerization of microtubules (Fig.

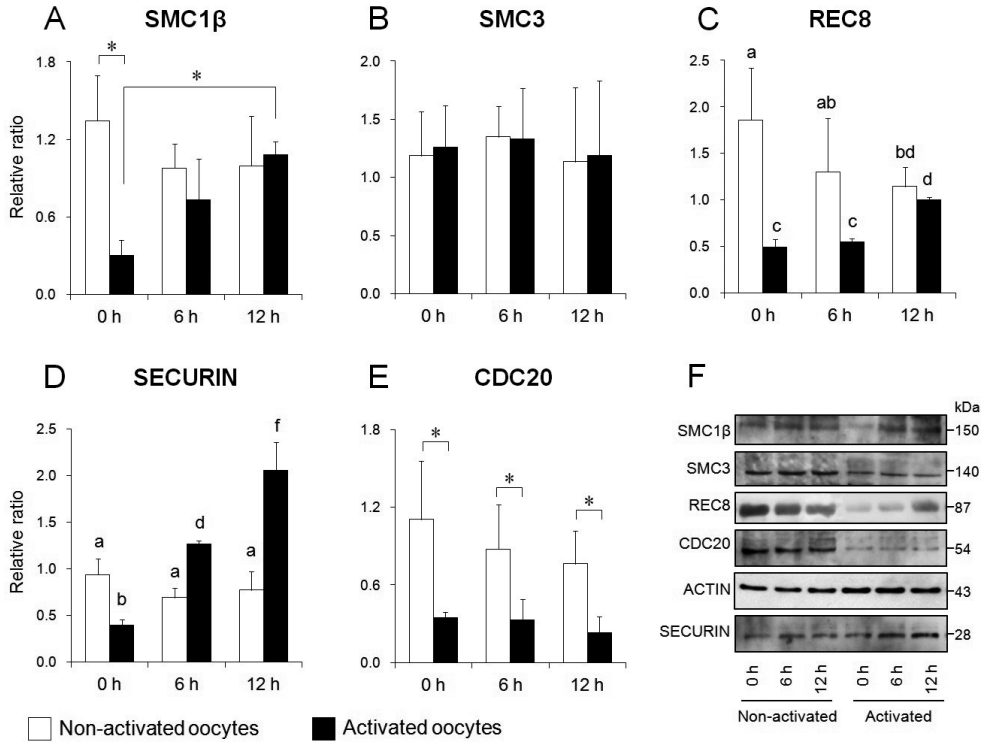

Fig. 6. Comparison of expression levels of cohesin subunits, securin and CDC20 in mouse oocytes. Relative expression of SMC1β (A), SMC3 (B), REC8 (C), securin (D), and CDC20 (E). (F) Western blotting for each protein in oocytes before (left) and after (right) activation. β-actin was used as a loading control. Bars with different superscripts indicate significant differences ($P < 0.05$). * $P < 0.05$.

4A). In the MII stage, the spindle of oocytes has a barrel shape, and the spindle fibers retain connections to the kinetochore on the chromosome aligned at the equator. When all kinetochores were fully connected to spindle fibers, the localization of MAD2 to the kinetochore was not observed. MII oocytes, where microtubule polymerization was inhibited by nocodazole treatment, exhibited no microtubule formation, and localized MAD2 expression at the kinetochore was detected. The expression level of MAD2 was shown as a ratio relative to β-actin expression. The expression level of MAD2 in the oocytes treated with nocodazole was 0.96 ± 0.13, and there was no difference compared to that observed in control oocytes (0.73 ± 0.12) (Fig. 4B).

Immunofluorescent staining results of MAD2 in 12 h aged oocytes are shown in Fig. 5. Despite the inhibition of spindle fiber connections to kinetochores on the misaligned chromosomes, MAD2 signals were not observed at some kinetochores (Fig. 5A). However, MAD2 localization was detected at kinetochores with fully connected spindles in 12 h aged oocytes (Fig. 5B). These results indicated that the system that monitors the connection between microtubules and kinetochores based on MAD2 localization might be disturbed by oocyte aging. The expression levels of MAD2 in the aged oocytes are shown in Fig. 5C. In non-activated oocytes (MII oocytes), the expression levels of MAD2 were 0.78 ± 0.20, and 0.94 ± 0.11 in the 6 and 12 h aged groups, respectively, and 0.73 ± 0.12 in the fresh group. In activated oocytes, the expression levels of MAD2 were 0.96 ± 0.14, 1.04 ± 0.14 in the 6 and 12 h aged groups, respectively, and 0.89 ± 0.03 in the fresh group. There were no significant differences between the aged groups and the fresh group, irrespective of oocyte activation status.

Expression of cohesin subunits, securin and CDC20

In this study, we assessed the cohesin complex as a terminal molecule in the SAC mechanism, and as a regulator of sister chromatid separation. The expression levels of SMC1β and SMC3 are shown in Fig. 6A, B, and F. In non-activated oocytes (MII oocytes), the expression levels of SMC1β are shown as a ratio, relative to β-actin expression, and were 0.98 ± 0.19 and 1.00 ± 0.39 in the 6 and 12 h aged groups, respectively. There were no significant differences between the aged groups and the fresh group (1.35 ± 0.35). In activated oocytes, the expression levels of SMC1β were 0.73 ± 0.32 and 1.08 ± 0.10 in the 6 and 12 h aged groups, respectively. SMC1β levels in the aged groups were higher than in the fresh group; in particular, there was a significant difference between the 12 h aged group and the fresh group (0.30 ± 0.12, $P < 0.05$) (Fig. 6A). As for the comparison of expression levels between before and after activation, SMC1β levels after activation were significantly lower than those before activation in fresh oocytes ($P < 0.05$). However, no significant difference was recognized between before and after activation in the aged oocytes. Concerning SMC3, the expression levels in non-activated oocytes were 1.35 ± 0.26 and 1.13 ± 0.64 in the 6 and 12 h aged groups, respectively, and 1.19 ± 0.38 in the fresh group. The expression levels in activated oocytes were 1.33 ± 0.44 and 1.19 ± 0.64 in the

6 and 12 h aged groups, respectively, and 1.26 ± 0.36 in the fresh group. In contrast to SMC1β, the expression levels of SMC3 were not different among groups, regardless of oocyte activation status (Fig. 6B). The expression levels of REC8 are shown in Fig. 6C and F. In non-activated oocytes, expression levels of REC8 were 1.30 ± 0.58 and 1.15 ± 0.21 in the 6 and 12 h aged groups, respectively. The REC8 levels of MII oocytes declined over time *in vitro*, with a significant difference between the 12 h aged group and the fresh group (1.86 ± 0.56, $P < 0.05$). In activated oocytes, the expression levels of REC8 were 0.55 ± 0.04 and 1.00 ± 0.03 in the 6 and 12 h aged groups, respectively. The REC8 level in the 12 h aged group was significantly higher than that in the other groups ($P < 0.05$). Comparing expression levels between before and after activation, REC8 abundance after activation was significantly lower than that before activation in fresh oocytes ($P < 0.05$). However, no significant difference was identified between before and after activation in aged oocytes.

Expression levels of securin are shown in Fig. 6D and F. In non-activated oocytes, the expression levels of securin were 0.69 ± 0.10 and 0.77 ± 0.20 in the 6 and 12 h aged groups, respectively. There were no significant differences between the aged groups and the fresh group (0.94 ± 0.17). In activated oocytes, the expression levels of securin were 1.26 ± 0.04 and 2.06 ± 0.30 in the 6 and 12 h aged groups, respectively. Securin levels in activated oocytes increased with age *in vitro*; there was a significant difference between the aged group and the fresh group (0.39 ± 0.06, $P < 0.05$). Comparing expression levels between before and after activation, securin levels after activation were significantly lower than before activation in fresh oocytes ($P < 0.05$). In contrast, securin levels after activation were significantly higher than before activation in the aged group ($P < 0.05$).

The expression levels of CDC20 are shown in Fig. 6E and F. In non-activated oocytes, the expression levels of CDC20 were 0.87 ± 0.35 and 0.76 ± 0.25 in the 6 and 12 h aged groups, respectively. The CDC20 levels in MII oocytes gradually decreased with age. However, no significant difference was recognized between the aged group and the fresh group (1.11 ± 0.45). In activated oocytes, the expression levels of CDC20 were 0.33 ± 0.16 and 0.23 ± 0.13 in the 6 and 12 h aged groups, respectively. No significant difference was recognized between the aged group and the fresh group (0.34 ± 0.05). Comparing expression levels between before and after activation, CDC20 levels after activation were significantly lower than before activation in all groups ($P < 0.05$).

Discussion

In our present study, three facts were revealed about the effect of post-ovulatory oocyte aging on meiosis II. First, it was established that NCAs are frequently induced in early embryos derived from *in vitro* aged oocytes, and these NCAs are due to errors in sister chromatid segregation that occurred during meiosis II. Second, it was shown that abnormalities in MAD2 localization, one of the checkpoint signal molecules that monitor the connections between spindle fiber and kinetochore, were found in aged MII oocytes. Finally, segregation errors were found on sister chromatids, which were attributed to the obstruction of appropriate cohesin subunit maintenance, and degradation in aged oocytes.

Ability of activated oocytes to form pronuclei tended to decrease with advancing aging time *in vitro*. The effects of *in vitro* aging on fertilization and preimplantation development seemed to appear by 12 h at the latest from oocyte collection. These results appeared to reflect the NCA frequencies in aged oocytes, or in embryos derived from aged oocytes, as described later. In this study, approximately 40% of the chromosome spreads analyzed from 8-cell embryos derived from 12 h aged oocytes exhibited aneuploidy (Fig. 2). Additionally, aneuploidy was detected in 12 h aged oocytes, which had completed second meiosis; this occurred at the same frequency as observed in 8-cell embryos. These data suggested that aneuploidy occurred more frequently in embryos derived from *in vitro* aged oocytes during early development, and that these aneuploidies originated from sister chromatid segregation errors during meiosis II. The major factor causing chromosomal aneuploidy in oocytes is abnormality of chromosome separation during meiosis [28, 29]. Many reports have suggested that failed chromosome distribution is caused by alterations in spindle shape and the misalignment of chromosomes at the equatorial plane in MII oocytes [11, 31, 32]. Normal spindles are barrel-shaped, including chromosomes, which are accurately aligned on the equator in mouse oocytes [8]. It has been indicated that, even when the spindle is normally shaped, it tends to elongate with the progress of aging *in vitro*. As shown in Fig. 3, aged oocytes obtained in the present study also had elongated spindles, which is consistent with the results of previous reports [30, 32]. Furthermore, some aged oocytes had obscured spindles and misaligned chromosomes, with no spindle fibers connected to the kinetochore. In aged oocytes, microtubules were gradually lost from the spindle, with the greatest loss in the central spindle area near the chromosome [8]. From these facts, it appeared that the obscure spindles and disrupted microtubules were caused by tubulin depolymerization. The poor connection between spindle fiber and chromosome kinetochore caused by microtubule disruption generates a disproportionate tension between the chromatids. In the second meiosis, when the spindle microtubules equally pull the sister kinetochores from the opposite poles, tension is generated between the sister chromatids, and the connection stabilizes [33, 34]. If the microtubules pull the sister kinetochores in the wrong direction, the connection is usually corrected and the sister chromatids are accurately distributed. By activating a checkpoint signal and blocking an advance to anaphase stage, SAC ensures that there is time to correct any connection errors between spindle fiber and kinetochore [35].

When SAC does not respond correctly to an improper connection of the spindle fibers to a kinetochore, the frequency of aneuploidy in aged oocytes may be increased [22, 23, 28, 36]. Thus, it is important to note that abnormalities in the localization of a checkpoint signal molecule were found in aged MII oocytes (Fig. 5). MAD2, which binds with MAD1 on the kinetochore, plays a role in monitoring the connection between spindle fibers and kinetochores [36–38]. MAD2 does not usually appear when connections between spindle fibers and kinetochores occur normally. However, when MII oocytes were treated with nocodazole, which is an inhibitor of microtubule polymerization, MAD2 was detected near the centromere (Fig. 4). In this study, it was revealed that some aged oocytes did not show MAD2 localization on the chromosome kinetochore, despite failed

spindle fiber-kinetochore connections. In contrast, other aged oocytes indicated MAD2 localization at kinetochores with spindle fiber connections. Zhang *et al*. have reported that MAD2 localization to a chromosome that was out of alignment on the equator might gradually dissipate [39]. Even if several chromosomes lacking a stable kinetochore-microtubule connection exist, these are not enough to prevent the advance to anaphase and the resulting chromosome distribution error [34, 40]. On the other hand, in research using murine or porcine oocytes, it has been reported that the expression level of MAD2 gradually decreased as oocytes aged [36, 41, 42]. Our data showed that there is no significant difference in the expression level of MAD2 between aged and fresh oocytes, regardless of oocyte activation. Because MAD2 exists in a free state, not only in the nucleus but also in the cytoplasm [36], data assessing increases or decreases in MAD2 expression do not address MAD2's role as a checkpoint signal. However, based on the combination of MAD2 localization data and expression levels, it is possible to discern a potential age-related dysfunction in the checkpoint system through which MAD2 monitors the kinetochore-microtubule connection.

Previous reports have provided distinct evidence that the deterioration of sister chromatid cohesion was a cause of age-related aneuploidy [21–25, 37]. The cohesin complex serves as an adhesion molecule connecting sister chromatids during chromosome segregation regulated by SAC. REC8, which is a meiosis-specific subunit of cohesin, has a separase recognition site that is specifically cleaved by separase [22]. Thus, the expression of cohesin REC8 is essential to retain proper sister chromatid connections until the terminal phase of chromosome segregation. It is known that *Rec8*-deficient mice show a loss of synapsis in homologous chromosomes, and poor cohesion of sister chromatids [21]. Even in wild-type mice, it was shown that REC8 gradually reduce on chromosome as mice age [21–23, 25, 43]. Chiang *et al*. [23] have reported that sister kinetochores in MI and MII oocytes from old mice are not tightly connected. They have also shown that, in oocytes with poor connections between sister kinetochores, REC8 expression levels decreased and sister chromatid cohesion was weakened. In human oocytes, the age-dependent deterioration of cohesin REC8 has been recognized, strongly suggesting an association with premature separation of sister chromatids (PSSC), which is a factor in aneuploidy [43]. Although previous findings are associated with maternal aging, in this study it has been revealed that, even in young mice, the time-dependent deterioration of REC8 occurred in MII oocytes that were aged *in vitro* after ovulation. Recent reports have suggested that the weak cohesion associated with the age-dependent decrease in REC8 was attributed to a gradual loss of Shugoshin (SGO1 and SGO2), which is a protector of cohesin [22]. In fission yeast, SGO1, which protects the limited cohesin in the centromere region from separase during meiosis I, enables the adhesion of sister chromatids until meiosis II. However, its expression is meiosis I-specific [44, 45], and it has been suggested that SGO2, which is expressed during both meiosis I and II, might be not directly involved in cohesin protection [44]. In mammals, it has been reported that both SGO1 and SGO2 localize around the inner kinetochore in both meiosis I and meiosis II [46]. This report also mentioned that SGO2 is highly expressed in oocytes, whereas expression of SGO1 is moderate. Moreover, analysis of RNA interference against *Sgo1* or *Sgo2* in MII oocytes has shown that REC8 is preserved at centromeres in *Sgo1*-depleted oocytes, but disappears in *Sgo2*-depleted oocytes. These facts suggest that *Sgo2* play a major role in centromere to protect REC8 from cleavage by separase. In fission yeast, it has been proposed that SGO2 localizes Aurora B kinase, which cancels misconnections of kinetochore-spindles, to the centromere and promotes the activation of SAC signals such as the localization of MAD2 to the kinetochore [44, 47]. Thus, the time-dependent deterioration of MII cohesin, and the errors in MAD2 localization in *in vitro* aged oocytes, might be related to the decrease in SGO2 expression. Our data indicated that post-ovulatory oocyte aging weakens sister chromatid cohesion, and might become a factor of PSSC, causing aneuploidy.

Surprisingly, the expression level of REC8 increased in activated oocytes, depending on aging time, and did not significantly change in aged oocytes after activation, as compared with aged oocytes before activation. The expression level of cohesin REC8 usually decreases promptly after activation. Securin, which is a suppressor of separase, was overexpressed in activated aged oocytes, which may be one of the reasons for disturbing the decrease in REC8. Securin is ubiquitinated in a CDC20-dependent manner via APC/C, and then degraded by proteasomes [48]. In our present study, there was no effect of post-ovulatory oocyte aging on the expression of CDC20, an activator of APC/C, regardless of oocyte activation. On the other hand, as is case with REC8, SMC1β decreased in MII aged oocytes, and did not significantly change in activated aged oocytes, as compared with oocytes before activation. Interestingly, SMC1β is also expressed specifically during meiosis and has been suggested as a potential cause of age-related aneuploidy [21, 22]. It is unclear why only the meiosis-specific subunits were affected by oocyte aging. This study is the first report to find that post-ovulatory aging obstructed cohesin decreases in activated oocytes. Our present data suggested that the maintenance of cohesin REC8 and SMC1β in aged oocytes after activation might lead to non-disjunction of sister chromatids during MII.

In conclusion, it was shown that the post-ovulatory aging of oocytes inhibited MAD2 localization to the kinetochore. Furthermore, post-ovulatory aging prevented cohesin subunit maintenance, or degradation, at the appropriate time. It was also suggested that destabilization of SAC signaling caused sister chromatid segregation errors in MII oocytes, and consequently increased the incidence of NCAs in early embryos. NCAs during early development are a cause for pregnancy loss, as well as being a major genetic origin of congenital deficiency [9, 20, 22]. Most NCAs originate in oocytes, and it has been widely acknowledged that maternal age is a principal risk factor for NCAs [23]. Our findings have provided distinct evidence that the post-ovulatory aging of oocytes might also become a risk factor for NCA development, irrespective of maternal age.

References

1. **Zhang D, Keilty D, Zhang ZF, Chian RC.** Mitochondria in oocyte aging: current understanding. *Facts Views Vis ObGyn* 2017; **9**: 29–38. [Medline]
2. **Bentov Y, Casper RF.** The aging oocyte—can mitochondrial function be improved? *Fertil Steril* 2013; **99**: 18–22. [Medline] [CrossRef]
3. **Takahashi T, Igarashi H, Kawagoe J, Amita M, Hara S, Kurachi H.** Poor embryo development in mouse oocytes aged in vitro is associated with impaired calcium homeostasis. *Biol Reprod* 2009; **80**: 493–502. [Medline] [CrossRef]

4. **Gordo AC, Rodrigues P, Kurokawa M, Jellerette T, Exley GE, Warner C, Fissore R.** Intracellular calcium oscillations signal apoptosis rather than activation in in vitro aged mouse eggs. *Biol Reprod* 2002; **66**: 1828–1837. [Medline] [CrossRef]
5. **Huang JC, Yan LY, Lei ZL, Miao YL, Shi LH, Yang JW, Wang Q, Ouyang YC, Sun QY, Chen DY.** Changes in histone acetylation during postovulatory aging of mouse oocyte. *Biol Reprod* 2007; **77**: 666–670. [Medline] [CrossRef]
6. **Ge ZJ, Schatten H, Zhang CL, Sun QY.** Oocyte ageing and epigenetics. *Reproduction* 2015; **149**: R103–R114. [Medline] [CrossRef]
7. **Liu L, Keefe DL.** Ageing-associated aberration in meiosis of oocytes from senescence-accelerated mice. *Hum Reprod* 2002; **17**: 2678–2685. [Medline] [CrossRef]
8. **Miao YL, Kikuchi K, Sun QY, Schatten H.** Oocyte aging: cellular and molecular changes, developmental potential and reversal possibility. *Hum Reprod Update* 2009; **15**: 573–585. [Medline] [CrossRef]
9. **Selesniemi K, Lee HJ, Muhlhauser A, Tilly JL.** Prevention of maternal aging-associated oocyte aneuploidy and meiotic spindle defects in mice by dietary and genetic strategies. *Proc Natl Acad Sci USA* 2011; **108**: 12319–12324. [Medline] [CrossRef]
10. **Nagy ZP, Rienzi LF, Ubaldi FM, Greco E, Massey JB, Kort HI.** Effect of reduced oocyte aging on the outcome of rescue intracytoplasmic sperm injection. *Fertil Steril* 2006; **85**: 901–906. [Medline] [CrossRef]
11. **Ono T, Mizutani E, Li C, Yamagata K, Wakayama T.** Offspring from intracytoplasmic sperm injection of aged mouse oocytes treated with caffeine or MG132. *Genesis* 2011; **49**: 460–471. [Medline] [CrossRef]
12. **Franasiak JM, Forman EJ, Hong KH, Werner MD, Upham KM, Treff NR, Scott RT.** Aneuploidy across individual chromosomes at the embryonic level in trophectoderm biopsies: changes with patient age and chromosome structure. *J Assist Reprod Genet* 2014; **31**: 1501–1509. [Medline] [CrossRef]
13. **Kaplan OL, Trounson A.** Reduced developmental competence of immature, in-vitro matured and postovulatory aged mouse oocytes following IVF and ICSI. *Reprod Biol Endocrin* 2008; **6**.
14. **Howe K, FitzHarris G.** Recent insights into spindle function in mammalian oocytes and early embryos. *Biol Reprod* 2013; **89**: 71. [Medline] [CrossRef]
15. **Kapanidou M, Lee S, Bolanos-Garcia VM.** BubR1 kinase: protection against aneuploidy and premature aging. *Trends Mol Med* 2015; **21**: 364–372. [Medline] [CrossRef]
16. **Shandilya J, Toska E, Richard DJ, Medler KF, Roberts SGE.** WT1 interacts with MAD2 and regulates mitotic checkpoint function. *Nat Commun* 2014; **5**: 4903. [Medline] [CrossRef]
17. **Peters JM, Tedeschi A, Schmitz J.** The cohesin complex and its roles in chromosome biology. *Genes Dev* 2008; **22**: 3089–3114. [Medline] [CrossRef]
18. **Garcia-Cruz R, Brieño MA, Roig I, Grossmann M, Velilla E, Pujol A, Cabero L, Pessarrodona A, Barbero JL, Garcia Caldés M.** Dynamics of cohesin proteins REC8, STAG3, SMC1 beta and SMC3 are consistent with a role in sister chromatid cohesion during meiosis in human oocytes. *Hum Reprod* 2010; **25**: 2316–2327. [Medline] [CrossRef]
19. **Tsutsumi M, Fujiwara R, Nishizawa H, Ito M, Kogo H, Inagaki H, Ohye T, Kato T, Fujii T, Kurahashi H.** Age-related decrease of meiotic cohesins in human oocytes. *PLoS One* 2014; **9**: e96710. [Medline] [CrossRef]
20. **Duncan FE, Hornick JE, Lampson MA, Schultz RM, Shea LD, Woodruff TK.** Chromosome cohesion decreases in human eggs with advanced maternal age. *Aging Cell* 2012; **11**: 1121–1124. [Medline] [CrossRef]
21. **Revenkova E, Adelfalk C, Jessberger R.** Cohesin in oocytes-tough enough for Mammalian meiosis? *Genes (Basel)* 2010; **1**: 495–504. [Medline] [CrossRef]
22. **Jessberger R.** Age-related aneuploidy through cohesion exhaustion. *EMBO Rep* 2012; **13**: 539–546. [Medline] [CrossRef]
23. **Chiang T, Duncan FE, Schindler K, Schultz RM, Lampson MA.** Evidence that weakened centromere cohesion is a leading cause of age-related aneuploidy in oocytes. *Curr Biol* 2010; **20**: 1522–1528. [Medline] [CrossRef]
24. **Yun Y, Holt JE, Lane SI, McLaughlin EA, Merriman JA, Jones KT.** Reduced ability to recover from spindle disruption and loss of kinetochore spindle assembly checkpoint proteins in oocytes from aged mice. *Cell Cycle* 2014; **13**: 1938–1947. [Medline] [CrossRef]
25. **Fu X, Cheng J, Hou Y, Zhu S.** The association between the oocyte pool and aneuploidy: a comparative study of the reproductive potential of young and aged mice. *J Assist Reprod Genet* 2014; **31**: 323–331. [Medline] [CrossRef]
26. **Yoshizawa M, Araki Y, Motoyama M.** Analyses of early development and chromosomal constitution of tripronuclear human and mouse eggs fertilization in vitro. *Jpn J Fertil Steril* 1997; **42**: 34–38 (In Japanese).
27. **Yoshizawa M, Konno H, Zhu S, Kageyama S, Fukui E, Muramatsu S, Kim S, Araki Y.** Chromosomal diagnosis in each individual blastomere of 5- to 10-cell bovine embryos derived from in vitro fertilization. *Theriogenology* 1999; **51**: 1239–1250. [Medline] [CrossRef]
28. **Jones KT.** Meiosis in oocytes: predisposition to aneuploidy and its increased incidence with age. *Hum Reprod Update* 2008; **14**: 143–158. [Medline] [CrossRef]
29. **MacLennan M, Crichton JH, Playfoot CJ, Adams IR.** Oocyte development, meiosis and aneuploidy. *Semin Cell Dev Biol* 2015; **45**: 68–76. [Medline] [CrossRef]
30. **Wakayama S, Thuan NV, Kishigami S, Ohta H, Mizutani E, Hikichi T, Miyake M, Wakayama T.** Production of offspring from one-day-old oocytes stored at room temperature. *J Reprod Dev* 2004; **50**: 627–637. [Medline] [CrossRef]
31. **Takahashi K, Matsui H, Takahashi I, Matsumoto H, Fukui E, Motoyama M, Yoshizawa M.** Effects of in vitro aging of mouse oocytes on metaphase II spindle morphology, in vitro fertilization and subsequent embryonic development. *J Mamm Ova Res* 2010; **27**: 42–50. [CrossRef]
32. **Lee AR, Shimoike T, Wakayama T, Kishigami S.** Phenotypes of aging postovulatory oocytes after somatic cell nuclear transfer in mice. *Cell Reprogram* 2016; **18**: 147–153. [Medline] [CrossRef]
33. **Lampson MA, Cheeseman IM.** Sensing centromere tension: Aurora B and the regulation of kinetochore function. *Trends Cell Biol* 2011; **21**: 133–140. [Medline] [CrossRef]
34. **Kitajima TS.** Cell biological causes of aneuploidy in eggs. *J Mamm Ova Res* 2017; **2**: 39–44. (In Japanese).
35. **Musacchio A.** Spindle assembly checkpoint: the third decade. *Philos Trans R Soc Lond B Biol Sci* 2011; **366**: 3595–3604. [Medline] [CrossRef]
36. **Vogt E, Kirsch-Volders M, Parry J, Eichenlaub-Ritter U.** Spindle formation, chromosome segregation and the spindle checkpoint in mammalian oocytes and susceptibility to meiotic error. *Mutat Res* 2008; **651**: 14–29. [Medline] [CrossRef]
37. **Jones KT, Lane SIR.** Molecular causes of aneuploidy in mammalian eggs. *Development* 2013; **140**: 3719–3730. [Medline] [CrossRef]
38. **Sun SC, Kim NH.** Spindle assembly checkpoint and its regulators in meiosis. *Hum Reprod Update* 2012; **18**: 60–72. [Medline] [CrossRef]
39. **Zhang D, Ma W, Li YH, Hou Y, Li SW, Meng XQ, Sun XF, Sun QY, Wang WH.** Intraoocyte localization of MAD2 and its relationship with kinetochores, microtubules, and chromosomes in rat oocytes during meiosis. *Biol Reprod* 2004; **71**: 740–748. [Medline] [CrossRef]
40. **Nagaoka SI, Hodges CA, Albertini DF, Hunt PA.** Oocyte-specific differences in cell-cycle control create an innate susceptibility to meiotic errors. *Curr Biol* 2011; **21**: 651–657. [Medline] [CrossRef]
41. **Steuerwald NM, Steuerwald MD, Mailhes JB.** Post-ovulatory aging of mouse oocytes leads to decreased MAD2 transcripts and increased frequencies of premature centromere separation and anaphase. *Mol Hum Reprod* 2005; **11**: 623–630. [Medline] [CrossRef]
42. **Ma W, Zhang D, Hou Y, Li YH, Sun QY, Sun XF, Wang WH.** Reduced expression of MAD2, BCL2, and MAP kinase activity in pig oocytes after in vitro aging are associated with defects in sister chromatid segregation during meiosis II and embryo fragmentation after activation. *Biol Reprod* 2005; **72**: 373–383. [Medline] [CrossRef]
43. **Keefe D, Kumar M, Kalmbach K.** Oocyte competency is the key to embryo potential. *Fertil Steril* 2015; **103**: 317–322. [Medline] [CrossRef]
44. **Kawashima SA, Tsukahara T, Langegger M, Hauf S, Kitajima TS, Watanabe Y.** Shugoshin enables tension-generating attachment of kinetochores by loading Aurora to centromeres. *Genes Dev* 2007; **21**: 420–435. [Medline] [CrossRef]
45. **Kitajima TS, Kawashima SA, Watanabe Y.** The conserved kinetochore protein shugoshin protects centromeric cohesion during meiosis. *Nature* 2004; **427**: 510–517. [Medline] [CrossRef]
46. **Lee J, Kitajima TS, Tanno Y, Yoshida K, Morita T, Miyano T, Miyake M, Watanabe Y.** Unified mode of centromeric protection by shugoshin in mammalian oocytes and somatic cells. *Nat Cell Biol* 2008; **10**: 42–52. [Medline] [CrossRef]
47. **Pinsky BA, Biggins S.** The spindle checkpoint: tension versus attachment. *Trends Cell Biol* 2005; **15**: 486–493. [Medline] [CrossRef]
48. **Pesin JA, Orr-Weaver TL.** Regulation of APC/C activators in mitosis and meiosis. *Annu Rev Cell Dev Biol* 2008; **24**: 475–499. [Medline] [CrossRef]